

STUDY ON IGNITION OF GASEOUS FUELS USING DIFFERENT TYPES OF REACTORS

Sebastian WERLE*

* Dr.; Faculty of Energy and Environmental Engineering, Silesian University of Technology,
Konarskiego 22, 44-100, Gliwice, Poland

*E-mail address: *Sebastian.werle@polsl.pl*

Received: 18.08.2010; Revised: 02.11.2010; Accepted: 03.11.2010

Abstract

Ignition delay is an important parameter in the most modern and advanced combustor concepts designed for low-NO_x emission. Ignition phenomenon and complete reaction of fuel are required to achieve combustion efficiency. Ignition delay studies have been conducted using a variety of different experimental methods, such as jet-stirred reactors JSR, continuous flow reactors (co-flow reactors, CFR), rapid compression machines RCM, constant volume bombs (chambers, CVB) and shock tubes. The present paper focuses on the present experimental results of methane and propane ignition in two types of reactor: constant volume chamber and co-flow reactor. A summary of recent experimental studies of ignition delay is also presented.

Streszczenie

Czas zwłoki zapłonu jest istotnym parametrem w większości zaawansowanych rozwiązań niskoemisyjnych technik spalania. Z punktu widzenia efektywności procesu, zapłon i jednoczesna kompletna reakcja paliwa z utleniaczem jest absolutną koniecznością. Czas zwłoki zapłonu może być badany eksperymentalnie przy użyciu różnych typów reaktorów, takich jak reaktory z mieszaniem (ang. jet-stirred reactors), reaktory przepływowe (ang. continuous flow reactors), maszyny natychmiastowego sprężu (ang. rapid compression machines), reaktory o stałej objętości (constant volume bombs) i rury uderzeniowe (ang. shock tubes). W pracy zaprezentowano wyniki badań zapłonu metanu i propanu w dwóch spośród wymienionych: reaktor o stałej objętości CVB i reaktor przepływowy CFR. Dokonano także przeglądu najnowszych badań związanych z analizą czasu zwłoki zapłonu gazowych paliw węglowodorowych w reaktorach różnego typu.

Keywords: Ignition; CVB; CFR, RCM; Shock tube; JSR; Methane; Propane.

1. INTRODUCTION

Ignition, which is one of the most important stages of combustion and directly affects combustion efficiency and emissions, has been the subject of many studies trying to elucidate the ignition characteristics. The most important quantity defining the dynamics of the working processes in a combustor is the ignition delay after the creation of conditions necessary for ignition. This parameter governs the operating characteristics of various technical devices (e.g. engines, gas turbines). Ignition delay time studies have been conducted using a variety of different experimental methods,

such as jet-stirred reactors JSR, continuous flow reactors CFR, rapid compression machines RCM, constant volume bombs CVB and shock tubes. Therefore, when comparing ignition delay time data from different studies, it is important to consider how the experimental method used in each study could affect the measured ignition time. For example, the definition of the ignition delay time is not unique; studies that utilize similar experimental installations may not necessarily employ the same definition for the ignition delay.

There has been a considerable amount of research on measuring the ignition delay under a variety of condi-

Table 1.
Summary of experimental condition for recent hydrocarbon ignition data

	Reactor	Φ	T, K	p, atm	z_{O_2} , %	Fuel	Ref.
1		0.50	1200-1700	3.0-450.0	21.00	methane	[1]
2		0.50	867-1534	11.0-530.0	21.00	n-pentane	[2]
3	S H O C K	0.70-1.30	1000-1350	16.0-40.0	21.00	methane	[5]
4		0.50-2.00	1230-1840	7.3-9.5	0.50-9.00	cyclopentane and cyclohexane	[7]
5		1.00	900-1400	16.0-40.0	19.04-19.13	methane, ethane and propane	[8]
6		0.50-1.50	800-2400	1.0-3.0	0.50-9.00	methane	[10]
7	T U B E	0.20-0.80	940-1080	1.0	16.00; 21.00; 51.00	propane	[11]
8		0.50-2.00	1520-2000	3.6-18.2	1.50-2.00	methane	[12]
		0.50-2.00	1270-1520	2.9-14.2	0.90-3.70	ethane	
	0.50-1.50	1375-1580	3.5-9.7	0.06-2.60	propane		
9		0.20-2.00	650-2000	1.0-60.0	0.12-21.00	iso-octane	[13]
10		0.30; 1.00	620-1180	10.0; 30.0; 50.0	21.00	n-heptane	[14]
12	J S R	1.00	773-1573	1.0	21.00	methane, ethane	[3]
13	C V B	0.14-1.68	773-973	1.0	21.00	methane	[4]
		0.17-4.04	773-973	1.0	21.00	propane	
14	B	0.50-1.43	960-1234	1.0	5.00; 10.00; 15.00; 21.00	methane	[16, 17]
		0.50-1.43	803-1055	1.0	5.00; 10.00; 15.00; 21.00	propane	
15		1.00	650-950	9.0-11.0	21.00	n-heptan n-pentane	[6]
16	R C M	0.80; 1.20	700-900	9.0-11.0	21.00	butane	[9]
17		0.20-2.00	650-2000	1.0-60.0	0.12-21.00	iso-octane	[13]
18		0.25-1.00	943-1027	12.0-23.0	9.00-21.00	iso-octane	[15]
19	C F R	0.50-1.43	530-630	1.0	21.00	propane	[17]

tions using several types of reactors. A selection of results from shock tubes, JSR, CVB, RCM and CFR work focused on hydrocarbon fuel ignition investigations collected by the author is presented in Table 1.

Among the methods used to analyze oxidation mechanisms, the shock tube technique has long been an important means of investigation.

A shock tube utilizes a shock wave to almost instantaneously ($< 1 \mu\text{s}$) compress a test mixture to a desired temperature and pressure. A diaphragm initially divides the shock tube into two sections – a dri-

ver section and a driven section. Figure 1 shows a scheme of a shock tube.

The driven section is initially filled with the test mixture, and the driver section is filled with a high-pressure driver gas (e.g., helium) until the pressure difference across the diaphragm causes its rupture. As the high-pressure driver gas expands into the driven section, a shock wave is formed and it travels down the length of the shock tube, and compresses the test gas. When the shock wave reaches the shock tube endwall, it is reflected back towards the driven sec-

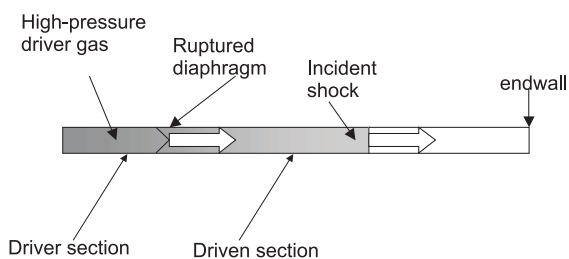


Figure 1.
Shock tube

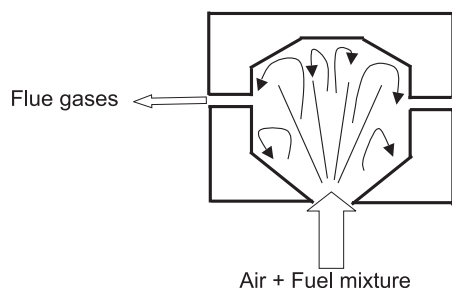


Figure 2.
Jet-stirred reactor

tion, which further compresses the test mixture. The test-time of most shock tubes is typically limited to under a few milliseconds, and therefore shock tube ignition time studies are often conducted at relatively high temperatures (>1000 K). From pressure signals or from the optical emission or absorption profiles of specific chemical species behind shock waves, the ignition delay can be obtained with good accuracy at high temperatures, without a wall effect.

An example of a jet-stirred reactor (JSR) is presented in Fig. 2.

This type of apparatus often consists of a ceramic cavity, into which a high speed jet of fuel and air is injected via a small nozzle. The fuel and air are typically premixed prior to entering the reactor. Impingement of the jet against the reactor wall causes vigorous mixing and recirculation of the gases which sustains the combustion process and creates a nearly homogeneous reaction zone. The ignition time in a JSR is determined by increasing the reactor loading (i.e., fuel-air mass flow rate) until the combustion is extinguished, which may be inferred from the sudden drop in the reactor temperature. The definition of the ignition time is based on the residence time in the reactor, calculated from the reactor volume, fuel-air mass flow rate, and the average gas density in the JSR [1].

Rapid compression machines (RCMs) have been

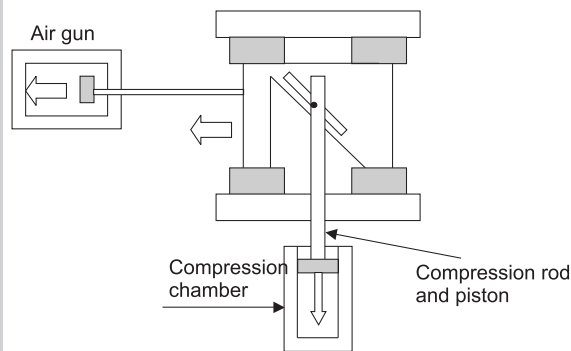


Figure 3.
Rapid compression machine

used for many years and provide a suitable environment for the study of hydrocarbon oxidation. The apparatus (see Fig. 3) provides a combustion chamber with a single piston stroke. The nature of the experiment, involving the compression of premixed gaseous fuel and oxidizer by a piston in a cylinder to a constant volume, takes the reactive charge through a temperature and pressure history similar to that in spark ignition engines.

In a continuous flow reactor (CFR), a blower and a preheater force a high-temperature stream of air through a long duct. Downstream of the preheater, the fuel is injected into the air stream through a nozzle.

A constant-volume bomb (CVB) is essentially an electrically-heated pressure vessel. It is initially filled with an oxygen-diluent mixture to a set pressure, and then heated to a prescribed temperature. A high-pressure nozzle then injects a fuel into the CVB, similarly by as in direct-injection automotive engines. The ignition time in a CVB is often defined as the time interval between the injection of the fuel and the initial rise in pressure that results from the combustion of the fuel.

In this investigation, the ignition of methane ($\text{CH}_4 > 98\%$) and propane ($\text{C}_3\text{H}_8 > 95\%$) using a high temperature oxidizer ($T > T_{\text{ai}}$) with varying oxygen concentration ($z_{\text{O}_2} = 0.05 \div 0.21$) was investigated, employing two types of experimental installation: constant-volume bomb (CVB) and co-flow reactor (CFR).

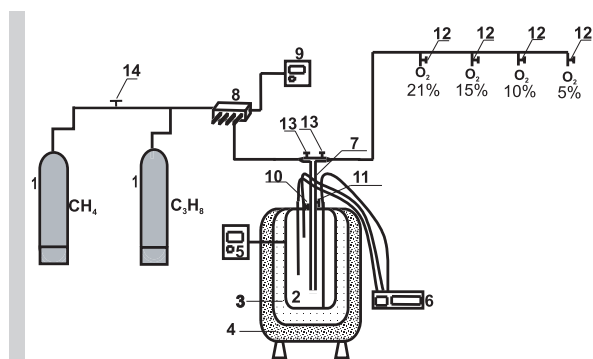


Figure 4.
Scheme of constant-volume bomb (CVB); 1 – gas cylinders, 2 – reaction chamber, 3 – heating coil, 4 – thermal insulation, 5 – microprocessor control unit, 6 – digital recorder, 7 – connecting tube, 8 – electric valve, 9 – control unit, 10 – safety vent, 11–14 – valves

2. EXPERIMENT

Fig. 4 shows the constant volume bomb.

The main part of the apparatus is a combustion chamber (2) (CVB) made of steel, of total volume approximately 400 cm^3 [17]. The oxidizers in the reaction cylinder were initially heated by heating coils (3) of total heating power 1.7 kW. Oxidizers with different oxygen concentrations were taken from gas cylinders (1), equipped with standard reducing valves and valves (12) to cut off the stream of oxidizer. The combustion chamber is insulated with ceramic fibre (4). Fuels from the appropriate gas cylinders (1) with reducing valve, through electric valve (8) (controlled by microprocessor control unit (9)) and connecting tube (7) were injected into the reaction chamber. Fuels at room temperature were injected into stationary oxidizer. Switching between both analyzed gases is done by opening and closing of valve (14). The tube supplying the fuel, of internal diameter 3 mm is equipped with four 0.5 mm holes situated around the axis of the tube. It is equipped with valves (11) and (13), which allow switching between dosing the oxidizer and fuel. In the upper cover there is a safety vent (10) as well as three holes, through which three thermoelements type S (PtRh10-Pt) are fitted and connected to a digital recorder (6). The temperature of the hot oxidizer inside the reaction chamber is controlled by a microprocessor control unit (5) integrated with a thermoelement of type K (NiCr-NiAl).

Fig. 5 shows co-flow reactor.

The reactor consists of ceramic chamber (2) heated by heating coils of total heating power 1.7 kW. The

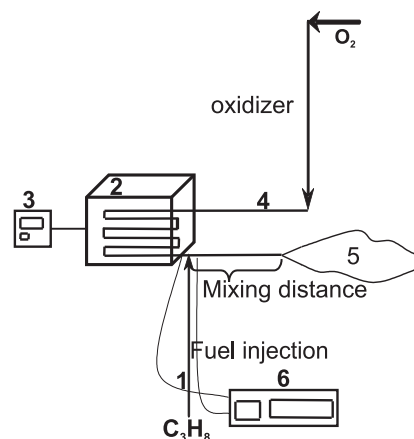


Figure 5.
Scheme of co-flow reactor (CFR), 1 – fuel and oxidizer injection, 2 – insulated reaction chamber, 3 – microprocessor control unit, 4 – stainless steel, spiral tube, 5 – flame, 6 – digital recorder

temperature inside the reaction chamber is controlled by a microprocessor control unit (3) integrated with a thermoelement of type K. Inside, the reactor chamber is fitted with a roll stainless steel, spiral tube (4) with an internal diameter 4 mm. Oxidizer (atmospheric air: $z_{\text{O}_2}=0.21$ and $z_{\text{N}_2}=0.79$) taken from a gas cylinder (1) passes through a heated pipe and initially preheated to the pre-set temperature. A stream of gas from cylinder (1), at room temperature, corresponding to set and controlled value of equivalence ratio is supplied to mix with the hot, flowing oxidizer. Ignition (and flame (5)) and the temperature rise recorded on a digital recorder (6) are observed.

The impact of the following variables: type of gaseous fuel, initial temperature of oxidizer T (for methane $T = 960 \div 1234 \text{ K}$ and for propane $T = 803 \div 1055 \text{ K}$), equivalence ratio $\varphi = 0.50 \div 1.43$ and volumetric composition of oxidizer (atmospheric air: $z_{\text{O}_2} = 0.21$ and $z_{\text{N}_2} = 0.79$, oxidizer 1: $z_{\text{O}_2} = 0.15$ and $z_{\text{N}_2} = 0.85$; oxidizer 2: $z_{\text{O}_2} = 0.10$ and $z_{\text{N}_2} = 0.90$; oxidizer 3: $z_{\text{O}_2} = 0.05$ and $z_{\text{N}_2} = 0.95$) on the ignition of methane and propane were investigated [17]. The full experimental matrix is presented in Table 2. An example of the way of determining the ignition delay τ_{ig} is presented in Fig. 6 [17]. Point “0” is interpreted as the moment of the injection of fuel and the start of the ignition procedure. The time from the moment of opening of the electric valve (point “0”) to the maximum temperature reached is taken as the ignition delay τ_{ig} . The maximum standard deviation of τ_{ig} is

Table 2.
Experimental matrix

Φ	CVB				CFR	
	methane		propane		propane	
	T, K	oxidizer	T, K	oxidizer	T, K	oxidizer
1.43	960, 989, 1005, 1034, 1055, 1085, 1104, 1134, 1186, 1206, 1234	1 – z _{O2} =0.21 & z _{N2} =0.79 2 – z _{O2} =0.15 & z _{N2} =0.85 3 – z _{O2} =0.10 & z _{N2} =0.90 4 – z _{O2} =0.05 & z _{N2} =0.95	803, 833, 853, 883, 903, 933, 960, 989, 1005, 1034, 1186	1 – z _{O2} =0.21 & z _{N2} =0.79 2 – z _{O2} =0.15 & z _{N2} =0.85 3 – z _{O2} =0.10 & z _{N2} =0.90 4 – z _{O2} =0.05 & z _{N2} =0.95	803, 833, 853, 883, 903	1 – z _{O2} =0.21 & z _{N2} =0.79
1.25	960, 989, 1005, 1034, 1055, 1085, 1104, 1134, 1186, 1206, 1234	1 – z _{O2} =0.21 & z _{N2} =0.79 2 – z _{O2} =0.15 & z _{N2} =0.85 3 – z _{O2} =0.10 & z _{N2} =0.90 4 – z _{O2} =0.05 & z _{N2} =0.95	803, 833, 853, 883, 903, 933, 960, 989, 1005, 1034, 1055	1 – z _{O2} =0.21 & z _{N2} =0.79 2 – z _{O2} =0.15 & z _{N2} =0.85 3 – z _{O2} =0.10 & z _{N2} =0.90 4 – z _{O2} =0.05 & z _{N2} =0.95	803, 833, 853, 883, 903	1 – z _{O2} =0.21 & z _{N2} =0.79
1.11	960, 989, 1005, 1034, 1055, 1085, 1104, 1134, 1186, 1206, 1234	1 – z _{O2} =0.21 & z _{N2} =0.79 2 – z _{O2} =0.15 & z _{N2} =0.85 3 – z _{O2} =0.10 & z _{N2} =0.90 4 – z _{O2} =0.05 & z _{N2} =0.95	803, 833, 853, 883, 903, 933, 960, 989, 1005, 1034, 1055	1 – z _{O2} =0.21 & z _{N2} =0.79 2 – z _{O2} =0.15 & z _{N2} =0.85 3 – z _{O2} =0.10 & z _{N2} =0.90 4 – z _{O2} =0.05 & z _{N2} =0.95	803, 833, 853, 883, 903	1 – z _{O2} =0.21 & z _{N2} =0.79
1.00	960, 989, 1005, 1034, 1055, 1085, 1104, 1134, 1186, 1206, 1234	1 – z _{O2} =0.21 & z _{N2} =0.79 2 – z _{O2} =0.15 & z _{N2} =0.85 3 – z _{O2} =0.10 & z _{N2} =0.90 4 – z _{O2} =0.05 & z _{N2} =0.95	803, 833, 853, 883, 903, 933, 960, 989, 1005, 1034, 1055	1 – z _{O2} =0.21 & z _{N2} =0.79 2 – z _{O2} =0.15 & z _{N2} =0.85 3 – z _{O2} =0.10 & z _{N2} =0.90 4 – z _{O2} =0.05 & z _{N2} =0.95	803, 833, 853, 883, 903	1 – z _{O2} =0.21 & z _{N2} =0.79
0.91	960, 989, 1005, 1034, 1055, 1085, 1104, 1134, 1186, 1206, 1234	1 – z _{O2} =0.21 & z _{N2} =0.79 2 – z _{O2} =0.15 & z _{N2} =0.85 3 – z _{O2} =0.10 & z _{N2} =0.90 4 – z _{O2} =0.05 & z _{N2} =0.95	803, 833, 853, 883, 903, 933, 960, 989, 1005, 1034, 1055	1 – z _{O2} =0.21 & z _{N2} =0.79 2 – z _{O2} =0.15 & z _{N2} =0.85 3 – z _{O2} =0.10 & z _{N2} =0.90 4 – z _{O2} =0.05 & z _{N2} =0.95	803, 833, 853, 883, 903	1 – z _{O2} =0.21 & z _{N2} =0.79
0.77	960, 989, 1005, 1034, 1055, 1085, 1104, 1134, 1186, 1206, 1234	1 – z _{O2} =0.21 & z _{N2} =0.79 2 – z _{O2} =0.15 & z _{N2} =0.85 3 – z _{O2} =0.10 & z _{N2} =0.90 4 – z _{O2} =0.05 & z _{N2} =0.95	803, 833, 853, 883, 903, 933, 960, 989, 1005, 1034, 1055	1 – z _{O2} =0.21 & z _{N2} =0.79 2 – z _{O2} =0.15 & z _{N2} =0.85 3 – z _{O2} =0.10 & z _{N2} =0.90 4 – z _{O2} =0.05 & z _{N2} =0.95	803, 833, 853, 883, 903	1 – z _{O2} =0.21 & z _{N2} =0.79
0.63	960, 989, 1005, 1034, 1055, 1085, 1104, 1134, 1186, 1206, 1234	1 – z _{O2} =0.21 & z _{N2} =0.79 2 – z _{O2} =0.15 & z _{N2} =0.85 3 – z _{O2} =0.10 & z _{N2} =0.90 4 – z _{O2} =0.05 & z _{N2} =0.95	803, 833, 853, 883, 903, 933, 960, 989, 1005, 1034, 1055	1 – z _{O2} =0.21 & z _{N2} =0.79 2 – z _{O2} =0.15 & z _{N2} =0.85 3 – z _{O2} =0.10 & z _{N2} =0.90 4 – z _{O2} =0.05 & z _{N2} =0.95	803, 833, 853, 883, 903	1 – z _{O2} =0.21 & z _{N2} =0.79
0.50	960, 989, 1005, 1034, 1055, 1085, 1104, 1134, 1186, 1206, 1234	1 – z _{O2} =0.21 & z _{N2} =0.79 2 – z _{O2} =0.15 & z _{N2} =0.85 3 – z _{O2} =0.10 & z _{N2} =0.90 4 – z _{O2} =0.05 & z _{N2} =0.95	803, 833, 853, 883, 903, 933, 960, 989, 1005, 1034, 1055	1 – z _{O2} =0.21 & z _{N2} =0.79 2 – z _{O2} =0.15 & z _{N2} =0.85 3 – z _{O2} =0.10 & z _{N2} =0.90 4 – z _{O2} =0.05 & z _{N2} =0.95	803, 833, 853, 883, 903	1 – z _{O2} =0.21 & z _{N2} =0.79

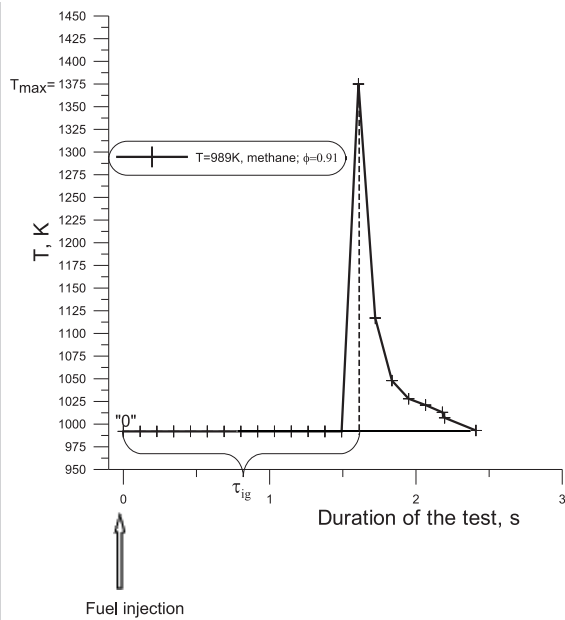


Figure 6.
Example of the ignition delay τ_{ig} as a function of the duration of the test

equal to $\sigma_{\tau_{ig}} = 0.017s$. The signals from thermocouples were collected every 0.001 s. The oxidizer temperature was measured with an enlarged uncertainty amounting $\delta T = 2K$ [18]. The error in the equivalence ratio $\delta\phi$ was equal to $\delta\phi = 0.02$.

3. RESULTS

In Fig. 7 the ignition delay τ_{ig} as a function of the oxidizer temperature T for both analyzed fuels and for equivalence ratio equal to $\phi = 0.91$ obtained in CVB reactor is shown.

It can be seen that for each test, as the oxidized temperature T is raised, the ignition delay initially decreases at the beginning with a growth of oxidizer temperature T . This is due to the fact that as the oxidizer temperature T increases the reaction rate and collision frequency of particles both increase. This figure shows that, there is a value of the oxidizer temperature T , for which the ignition delay reaches a minimum. As can be observed, for the value of T in which $\tau_{ig} = \tau_{min}$, the ignition delay for propane is lower than that for methane. As it is generally known, more complicated chemical complex structure of the propane molecule favors the easier ignition of propane than in methane. Above the T value at which the ignition delay reaches its minimum, this parameter increases due to lower level of density (concentration)

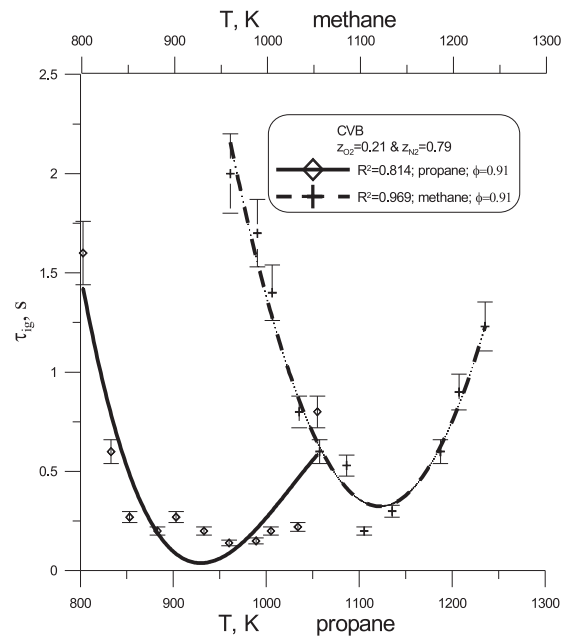


Figure 7.
Dependence of the ignition delay τ_{ig} as a function of oxidizer temperature T

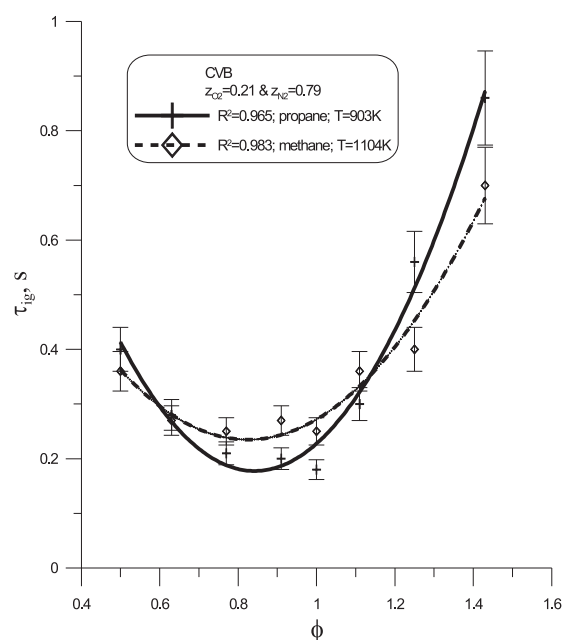


Figure 8.
Dependence of ignition delay τ_{ig} as a function of equivalence ratio ϕ

of the reacting gases at constant pressure (the chamber is not hermetic). It can be concluded, that despite the fact that increased oxidizer temperature T favors of growth reaction rates, the effect of falling gas density is much stronger. As a result, above

the T value at which $\tau_{ig} = \tau_{min}$, this parameter increases. It seems that preheating the oxidizer above this value of temperature oxidizer equal approximately to: in the case of methane $T \approx 1100$ K and in the case of propane $T \approx 950$ K is unsubstantiated. Similar diagrams have been plotted for all analyzed (see Table 2) values of the equivalence ratio but it is well known that most combustion properties have simple minima in the neighborhood of $\phi = 1$.

Fig. 8 shows the ignition delay as a function of the equivalence ratio for both analyzed fuels and for $T = 903$ K (in the case of propane) and for $T = 1104$ K (in the case of methane).

The evolution of τ_{ig} with Φ can be described by three branches, thereafter qualified as:

1. very lean: $\Phi \leq 0.15$,
2. lean, up to stoichiometric: $\Phi \in [0.15, 1.0]$,
3. rich: $\Phi > 1.0$.

Methane and propane as the majority of alkanes inhibit their own ignition [19] when the rate of chain branching (an essential process for combustion process) is higher than the rate of chain termination. Hydrogen atoms $^{\circ}H$ and alkyl radicals (the most important products of chain branching) under different conditions are characterized by different properties. It can be noticed in Fig. 8, that for rich mixtures ($\phi > 1$), alkanes are inhibitors of the ignition reaction due to important rerouting of hydrogen atoms from the chain branching reaction. This feature is predominating over ignition so ignition delay increases with growth of ϕ . For lean mixtures ($\phi < 1$), less frequent collisions between oxidizing and reducing species (small presence of fuel) limit the rerouting of hydrogen atoms (favorable factor). Here alkanes favour their own ignition. In this case, ignition delay decreases with growth of the ϕ . For values ϕ for which τ_{ig} reaches its minimum, there is a balance between amount of reactive radicals and hydrogen atoms.

In Fig. 9 it can be clearly observed that increment of oxygen concentration z_{O_2} in the oxidizer results in line decrease of τ_{ig} . The curves course is true for qualitative and characteristic changes rather than concrete values of analysed parameters. Tests with propane were characterized by lower values of ignition delay time τ_{ig} in comparison with methane.

Fig. 10 shows a comparison of the results obtained in CVB and CFR.

This diagram illustrates the dependence of the ignition delay τ_{ig} on the equivalence ratio. The main task

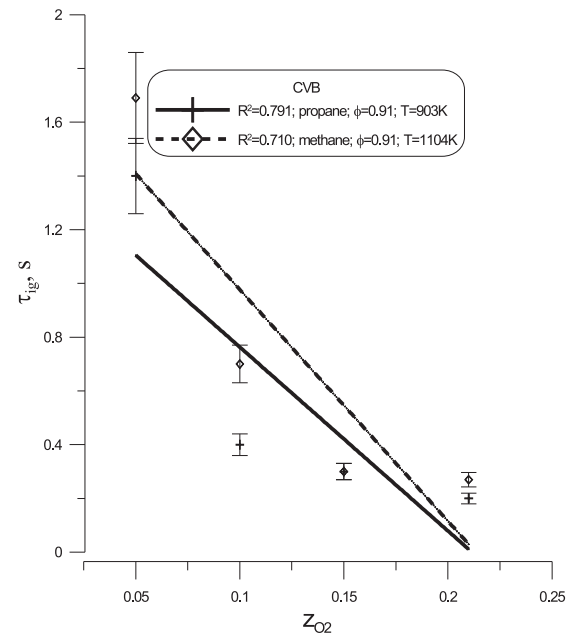


Figure 9. Ignition delay τ_{ig} as a function of molar fraction of oxygen in oxidizer z_{O_2}

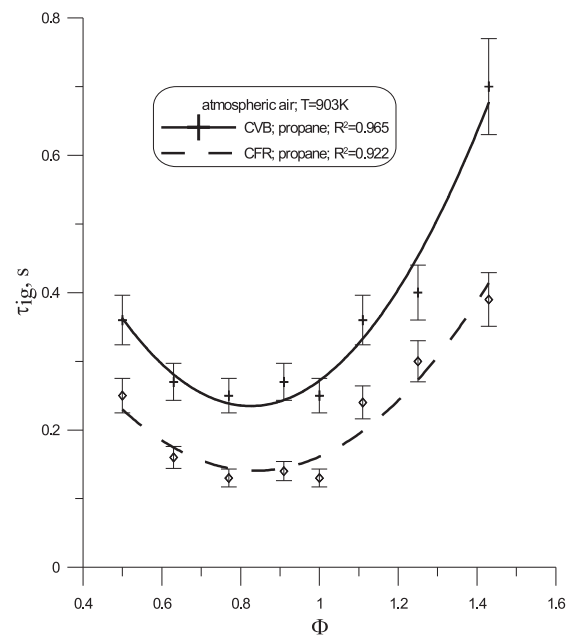


Figure 10. Ignition delay τ_{ig} as a function of equivalence ratio – comparison of CVB and CFR reactors

of research on CFR reactor was to test the technology in conditions similar to these in actual industrial furnaces and to compare the results obtained at different conditions of combustion (CVB and CFR reactors). It can be clearly noticed that CFR leads to

lower values of τ_{ig} , caused mainly by a much higher level of turbulence and a better homogeneity of the mixture. The results achieved with CFR confirm the conclusions drawn with CVB reactor. So it is possible to transfer the results obtained in CVB to CFR, which can be representative of furnace conditions.

4. CONCLUSION

In order to achieve the minimum ignition delay τ_{ig} (the maximum reaction rate) the oxidizer has to be preheated to a temperature of $T = 1100\text{K}$ (in the case of methane) and $T = 950\text{K}$ (in the case of propane). It seems that preheating of the oxidizer above these values is unsubstantiated. Additionally it is important to keep interval of equivalence ratio approximately equal to 0.9. Beyond this interval of T and φ in which $\tau_{ig} \rightarrow \min$, the parameter must increase. It is mainly caused by the smaller level of gas concentration in constant pressure conditions.

An increase in the oxygen concentration z_{O_2} in the oxidizer results in a linear decrease of τ_{ig} . Tests with propane were characterized by lower values of the ignition delay ig in comparison with methane.

The optimum value of the oxidizer temperature is probably a function of the combustion chamber type, the intensity of mixing and other factors. However, the experiments in the CFR suggest that it is probably possible to transfer results from the CVB reactor to practical installations.

REFERENCES

- [1] Zhukov V.P, Sechenov V.A., A. Starikovskii A.Yu.; Spontaneous ignition of methane-air mixtures in a wide range of pressure. *Combustion, Explosion and Shock Waves*, 39, 2003; p.487-495
- [2] Zhukov V.P, Sechenov V.A., A. Starikovskii A.Yu.; Self-ignition of a lean mixture of n-pentane and air over a wide range of pressures. *Combustion and Flame*, 140, 2005; p.196-230
- [3] Barbe P., Battin-Leclerc F., Come G.M.; Experimental and modeling study of methane and ethane oxidation between 773 and 1573 K. *J.Chem.Phys*, 92, 1995; p.1666-1692
- [4] Kong D., Eckhoff R.K., Alfret F.; Auto-ignition of CH_4/air , $\text{C}_3\text{H}_8/\text{air}$, $\text{CH}_4/\text{C}_3\text{H}_8/\text{air}$ and $\text{CH}_4/\text{CO}_2/\text{air}$ using a 1 l ignition bomb. *Journal of Hazardous Materials*, 40, 1995; p.69-84
- [5] Huang J., Hill P.G., Bushe W.K., Munshi S.R.; Shock-tube study of methane ignition under engine-relevant conditions: experiments and modeling. *Combustion and Flame*, 136, 2004; p.25-42
- [6] Mohamed C.; Suppression of reaction during rapid compression and its effect on delay, *Combustion and Flame*. 112, 1998; p.438-444
- [7] Sirjean B., Buda F., Hakka H., Glaude P.A., Fournet R., Warth V., Battin-Leclerc F., Ruiz-Lopez M.; The autoignition of cyclopentane and cyclohexane in a shock tube. *Proceedings of the Combustion Institute*, 31, 2007; p.277-284
- [8] Huang J., Bushe W.K.; Experimental and kinetic study of autoignition in methane/ethane/air and methane/propane/air mixtures under engine relevant conditions. *Combustion and Flame*, 144, 2006; p.74-88,
- [9] Minetti R., Ribaucour M., Carlier M., Fittschen C., Sochet L.R.; Experimental and modeling study of oxidation and autoignition of butane at high pressure. *Combustion and Flame*, 96, 1994; p.201-211
- [10] Cheng R.K., Oppenheim A.K.; Autoignition in methane-hydrogen mixtures. *Combustion and Flame*, 58, 1984; p.125-139
- [11] Freeman G., Lefebvre A.H.; Spontaneous ignition characteristic of gaseous hydrocarbon-air mixtures. *Combustion and Flame*, 58, 1984; p.153-162
- [12] Lamoureux N., Paillard C.-E., Vaslier V.; Low hydrocarbon mixtures ignition delay times investigation behind reflected shock waves. *Shock waves*, 11, 2002; p.309-322
- [13] Scott Goldsborough S.; A chemical kinetically based ignition delay time correlation for iso-octane covering a wide range of conditions including the NTC region. *Combustion and Flame*, 156, 2009; p.1248-1262
- [14] Herzler J., Fikri M., Hitzbleck K., Strake R., Schulz C., Roth P., Kalghatgi G.T.; Shock-tube study of the igni-

- tion of n-heptane/toluene/air mixtures at intermediate temperatures and high pressures. *Combustion and Flame*, 149, 2007; p.25-31
- [15] *He X., Donovan M.T., Zigler B.T., Palmer T.R., Walton S.M., Wooldridge M.S., Atreya A.*; An experimental and modeling study of iso-octane ignition delay times under homogeneous charge compression ignition conditions. *Combustion and Flame*, 142, 2005; p.266-275
- [16] *Werle S., Wilk R.K.*; A self-ignition of methane in high temperature air. *Chemical and Process Engineering*, 28, 2007; p.399-412
- [17] *Werle S., Wilk R.K.*; Ignition of methane and propane in high-temperature oxidizers with various oxygen concentrations. *Fuel*, 89, 2010; p.1833-1839
- [18] Agilent 34970A Data Acquisition/Switch Unit, Hewlett-Packard, 1999
- [19] *Imbert B., Lafosse F., Catoire L., Paillard C-E., Khasainov B.*; Formulation reproducing the ignition delays simulated by a detailed mechanism: Application to n-heptane combustion. *Combustion and Flame*, 155, 2008; p.380-408

NOMENCLATURE

p pressure [atm],
 R correlation coefficient,
 T temperature [K],
 z molar fraction of gas.

Greek letters:

δ uncertainty of measurement,
 σ standard deviation,
 φ equivalence ratio,
 τ time [s].

Subscripts

ai autoignition,
 ig ignition,
 min minimum.

